arXiv:1402.2639v1 [cond-mat.supr-con] 11 Feb 2014

Effect of the pseudogap on T_c in the cuprates and implications for its origin

Vivek Mishra[1], U. Chatterjee[2], J. C. Campuzano[1,3], and M. R. Norman[1*]
[1]*Materials Science Division, Argonne National Laboratory, Argonne, IL 60439*
[2]*Department of Physics, University of Virginia, Charlottesville, VA 22904*
[3]*Department of Physics, University of Illinois, Chicago, IL 60607*

(Dated: February 12, 2014)

Abstract

One of the most intriguing aspects of cuprates is a large pseudogap coexisting with a high superconducting transition temperature. Here, we study pairing in the cuprates from electron-electron interactions by constructing the pair vertex using spectral functions derived from angle resolved photoemission data for a near optimal doped $Bi_2Sr_2CaCu_2O_{8+\delta}$ sample that has a pronounced pseudogap. Assuming that that the pseudogap is *not* due to pairing, we find that the superconducting instability is strongly suppressed, in stark contrast to what is actually observed. Using an analytic approximation for the spectral functions, we can trace this suppression to the destruction of the BCS logarithmic singularity from a combination of the pseudogap and lifetime broadening. Our findings strongly support those theories of the cuprates where the pseudogap is instead due to pairing.

The origin of high temperature superconductivity remains one of the most intriguing problems in physics. A particularly dramatic observation in the cuprates is the presence of a large pseudogap that spans much of the doping-temperature phase diagram[1,2]. The origin of this pseudogap is as debated as the mechanism for superconductivity. In one class of theories, the pseudogap arises from some instability not related to pairing, typically charge, spin, or orbital current ordering. Recent evidence for this has come from a variety of measurements indicating symmetry breaking[3–6]. On the other side is a class of theories where the pseudogap is associated with pairing. This ranges from preformed pairs[7] to strong coupling 'RVB' theories where singlet spin pairs become charge coherent[8]. To date, numerical simulations, even on simple models such as the single band Hubbard and t-J models, have yet to definitively rule out one class in favor of the other.

For conventional superconductors, the development of the strong coupling Eliashberg approach[9] led to a detailed proof that the electron-phonon interaction was the cause of superconductivity. These equations could be inverted to derive the spectral function of the bosons responsible for the pairing, and this spectrum matched the phonon spectrum observed in the material[10]. Such methods have been employed as well in cuprates[11], but remain controversial since the strong momentum dependence of the interaction (responsible for the d-wave pairing) invalidates the approach used by McMillan and Rowell[10] based on tunneling data, which by definition are momentum averaged. This is in turn greatly complicated by the strongly anisotropic pseudogap, since the underlying assumption is a gapless normal state with weak momentum dependence. Here, we address this issue by directly using angle resolved photoemission (ARPES) data to construct the pair vertex. Under the assumption that the pseudogap is unrelated to pairing, we find no superconducting instability. We trace this effect to the suppression of the BCS logarithmic instability by the pseudogap itself.

To construct the pair vertex, we must first know the single particle Green's function. An issue is that ARPES only measures occupied states. As in earlier work, we surmount this difficulty under the assumption of particle-hole symmetry with respect to the Fermi energy and Fermi surface (k_F)

$$A(k,\omega) = I(k,\omega) + I(-k+2k_F,-\omega) \tag{1}$$

where I is the photoemission intensity and ω is measured relative to the chemical potential. Relaxing this approximation should only lead to minor differences in the results. The

assumption that the left hand side of the equation can be equated to the spectral function (imaginary part of the single particle Green's function) requires subtracting any background from the intensity (obtained from data for unoccupied momenta well beyond k_F), and then normalizing by requiring the integrated weight over frequency to be equal to unity. A similar method has been successfully employed by us in several works, most recently[12] to construct the dynamic susceptibility in cuprates, which was found to be in good agreement with inelastic neutron scattering (INS) data. In fact, the data set we employ here, from a near optimal doped $Bi_2Sr_2CaCu_2O_{8+\delta}$ sample with a T_c of 90 K, was used in that work to reproduce the momentum and energy dependence of the INS data in the superconducting state, in particular the unique hourglass-like dispersion observed in a variety of cuprates. In our case, though, we will use normal state data above T_c. For this sample, a relatively complete momentum sweep was done in an octant of the Brillouin zone at a temperature of 140 K[13], with data obtained on a 2 meV energy grid down to 322 meV below the Fermi energy, with the background intensity adjusted to match each spectrum at this lower energy cut-off.

To proceed, we will assume that pairing originates from electron-electron interactions. Although the particular approach used here is based on spin fluctuations, we believe the results are general to any electronic pairing mechanism. This first requires constructing the polarization bubble

$$\chi_0(q,\Omega) = \int_{-\infty}^{\infty} d\omega \int_{-\infty}^{\infty} d\omega' \frac{f(\omega) - f(\omega')}{\omega - \omega' + \Omega + i0^+} \frac{1}{N} \sum_k A(k+q,\omega) A(k,\omega') \tag{2}$$

with $f(\omega)$ the Fermi function and N the number of k points. The k sum is restricted to two dimensions under the further assumption of a single band (for the data set we use, there is no evidence for bilayer splitting). We will then make the standard random phase approximation to construct the full dynamic susceptibility

$$\chi(k,\Omega) = \frac{\chi_0(k,\Omega)}{1 - U\chi_0(k,\Omega)} \tag{3}$$

where U is an effective screened Hubbard interaction appropriate for a single band involving hybridized copper 3d and oxygen 2p orbitals.

In Fig. 1, we show the imaginary part of χ for two different values of U along the $(0,0) - (\pi,\pi)$ direction. For the larger value of U (860 meV), Im χ is concentrated at low frequencies at the commensurate wavevector (π,π). This is typical of very underdoped samples near the commensurate antiferromagnetic phase[14]. We contrast this with a smaller value of U

(800 meV), where spectral weight is now concentrated at incommensurate wavevectors at a higher energy, being a more appropriate description of INS data[15] for slightly underdoped samples (consistent with the ARPES data set employed). Decreasing U even further reduces the magnitude of Im χ, moves the incommensurate weight to even higher energies, and suppresses the lower energy commensurate weight.

Using this χ, the resulting electron-electron interaction is[16,17]

$$V(k,\Omega) = \bar{U}^2 \left[\frac{3}{2}\chi(k,\Omega) - \frac{1}{2}\chi_0(k,\Omega) \right] \tag{4}$$

where $\bar{U}$ differs from U because of vertex corrections[18]. To set $\bar{U}$, we will require that the renormalized Fermi velocity at the d-wave node (the Fermi surface along the $(0,0)-(\pi,\pi)$ direction) matches that determined from the ARPES dispersion (1.6 eV$\mathring{A}$) assuming a bare velocity of 3 eV$\mathring{A}$ from band theory. The renormalization factor (3/1.6) can be obtained as

$$Z = \left[1 - \frac{\partial \Sigma'}{\partial \omega} \right]_{\omega=0} \tag{5}$$

where Σ' is the real part of the fermion self-energy, and we assume Z arises from the same interaction V as above:

$$\Sigma(k, i\omega_n) = T \sum_{q,\omega_m} V(k-q, i\omega_n - i\omega_m) G_0(q, i\omega_m) \tag{6}$$

where G_0 is the bare fermion Green's function

$$G_0^{-1}(k, i\omega_n) = i\omega_n - \xi_k \tag{7}$$

and ξ_k is the bare dispersion (obtained from a tight binding fit to the ARPES dispersion by multiplying by the renormalization factor 3/1.6 mentioned above). The real part of Σ is then obtained by analytic continuation. For the case shown in Fig. 1a, $\bar{U}$ turns out to be the same as U. But for the case shown in Fig. 1b, we must increase $\bar{U}$ to 928 meV to obtain the same Z.

We now turn to the pairing problem. The anomalous (pairing) self-energy in the singlet channel is[16,17]

$$-\frac{T}{N} \sum_{k',\omega_m} V(k-k', i\omega_n - i\omega_m) \mathcal{P}_0(k', i\omega_m) \Phi(k', i\omega_m) = \Phi(k, i\omega_n) \tag{8}$$

with the pairing kernel $\mathcal{P}_0$

$$\mathcal{P}_0(k', i\omega_m) = G(k', i\omega_m) G(-k', -i\omega_m). \tag{9}$$

It is numerically convenient to solve this 'linearized' gap equation in the Matsubara representation (see Supplementary Information)

$$\mathcal{F}(k, i\omega) = -\int_{-\infty}^{+\infty} \frac{dx}{\pi} \frac{\mathcal{F}''(k,x)}{i\omega - x}, \tag{10}$$

where ω is the bosonic (fermionic) Matsubara frequency, for a given bosonic (fermionic) function $\mathcal{F}$. In Eq. (9), G is the fully dressed Green's function, which is formally determined by including the self-energy correction Eq. (6) in a completely self-consistent approach. Instead, we obtain G from the experimental spectral functions as discussed above using Eq. (10). This is related to the approach of Dahm *et al*[19] where INS data were used instead.

At T_c, the maximum eigenvalue (λ_{max}) of Eq. (8) reaches unity and the corresponding eigenvector gives the energy-momentum structure of the superconducting order parameter. Ideally, we would need to know G at each temperature. This is impractical when using real experimental data. Instead, we use our experimental normal state data at 140 K, and assume that all temperature dependence arises from the Matsubara frequencies. As we will see below, this is a best case scenario, since if anything, the magnitude of the pseudogap increases as the temperature is lowered.

Our results are shown in Fig. 2, labeled as FBZ (full Brillouin zone). We see that λ_{max} (which occurs for B_{1g}, i.e., d-wave, symmetry) is much less than unity and essentially temperature independent for both cases shown in Fig. 1. This implies that there is no superconductivity. This is the central result of our paper.

To understand this surprising result, we now turn to Fermi surface restricted calculations, which is a commonly employed approximation where the momentum perpendicular to the Fermi surface ($k_\perp$) is integrated out. This approximation is equivalent to ignoring the dependence of V on $k_\perp$. This procedure results in an equation which depends only on the angular variation around the Fermi surface:

$$-\frac{T}{N_\phi} \sum_{\phi', \omega_m} V_{nm}^{\phi\phi'} \mathcal{P}_0(\phi', i\omega_m) \Phi(\phi', i\omega_m) = \Phi(\phi, i\omega_n) \tag{11}$$

where N_ϕ is the number of angular points and $V_{nm}^{\phi\phi'}$ is

$$V_{nm}^{\phi\phi'} = V(k_{Fx}^{\phi} - k_{Fx}^{\phi'}, k_{Fy}^{\phi} - k_{Fy}^{\phi'}, i\omega_n - i\omega_m). \tag{12}$$

$\mathcal{P}_0$ is obtained by numerically integrating Eq. (9) using the experimental G over $k_\perp$, with the integration direction for each angle ϕ determined from the normal given by the tight binding fit to the ARPES data (this same procedure is used to identify k_F in Eq. (1)).

The results are also shown in Fig. 2. Although λ_{max} is now temperature dependent, over the temperature range shown, it is still below unity. Paradoxically, λ_{max} increases with increasing temperature. We have verified that at even higher temperatures, λ_{max} reaches a maximum, and then begins to fall, with the more realistic second case (Fig. 1b) always remaining below unity. Similar behavior for the T dependence of λ was reported by Maier *et al*[20].

To understand this behavior, we now turn to some analytic calculations. To a good approximation, we can approximate V for the d-wave case in the weak coupling BCS limit as

$$V(\phi, \phi') = \mathcal{V} \cos(2\phi) \cos(2\phi') \tag{13}$$

and assume an isotropic density of states N_0 over the Fermi surface coming from ξ_k. The weak coupling equation for T_c is

$$T \sum_{\omega_n} \int_0^{2\pi} \frac{d\phi}{2\pi} \mathcal{V} \cos^2(2\phi) P_0(\phi, i\omega_n) = 1. \tag{14}$$

For G we use a phenomenological form that is a good representation of ARPES data[21]

$$G(k, i\omega_n) = -\frac{i\omega_n + i\Gamma sgn(\omega_n) + \xi_k}{(\omega_n + \Gamma sgn(\omega_n))^2 + \xi_k^2 + \Delta_k^2}. \tag{15}$$

Here Γ is the broadening and Δ_k the anisotropic pseudogap, which consistent with ARPES, is assumed to have a d-wave anisotropy. On the Fermi surface, this can be approximated as $\Delta_0 \cos(2\phi)$. The pairing kernel can now be analytically derived

$$\mathcal{P}_0(\phi, i\omega_n) = \pi N_0 \left[\frac{1}{\sqrt{\tilde{\omega}_n^2 + \Delta_\phi^2}} - \frac{\Delta_\phi^2}{2(\tilde{\omega}_n^2 + \Delta_\phi^2)^{3/2}} \right]. \tag{16}$$

Here $\tilde{\omega}_n$ is $\omega_n + sgn(\omega_n)\Gamma$. To obtain an analytic approximation, we replace the sum $T \sum_{\omega_n}$ by an integral $\int d\omega/2\pi$, using the Euler-Maclaurin formula[22] for low temperatures in Eq. (14) and rewrite the condition for T_c as

$$1 = N_0 \mathcal{V} \int_{\pi T}^{\infty} d\omega \int_0^{2\pi} \frac{d\phi}{2\pi} \cos^2 2\phi \left[\frac{1}{\sqrt{\tilde{\omega}^2 + \Delta_\phi^2}} - \frac{\Delta_\phi^2}{2(\tilde{\omega}^2 + \Delta_\phi^2)^{3/2}} \right]. \tag{17}$$

The integral over ω can be carried out analytically. The second term is convergent, so we can integrate it to ∞. For the first term, we use a BCS cut-off energy ω_c and we assume

$\omega_c \gg T, \Delta_0, \Gamma$ and in the low T limit we get

$$1 \simeq N_0 \mathcal{V} \int_0^{2\pi} \frac{d\phi}{2\pi} \cos^2 2\phi \left[\log \left(\frac{1}{\sqrt{e}} \frac{2\omega_c}{\Gamma + \pi T + \sqrt{(\Gamma + \pi T)^2 + \Delta_\phi^2}} \right) + \frac{\Gamma + \pi T}{2\sqrt{(\Gamma + \pi T)^2 + \Delta_\phi^2}} \right]. \tag{18}$$

By examining Eq. (18), we can clearly see that the logarithmic divergence of the first term is cut-off by both Γ and Δ_0, so a solution is no longer guaranteed. We can estimate the critical values of the inverse lifetime and pseudogap to kill superconductivity at T=0 for limiting cases. In the clean limit with $\Gamma = 0$, $\Delta_{cri} = 2\pi e^{-(\gamma+1)} \mathrm{T}_{c0}$ where γ is Euler's constant and T_{c0} is T_c for $\Delta_0, \Gamma = 0$. With no pseudogap, we find a critical inverse lifetime Γ_{cri} of $\pi e^{-\gamma} T_{c0}/2$ (Abrikosov-Gor'kov[23]). Fig. 3 shows the numerically evaluated left hand side of Eq. (14) (denoted as λ_{max}^{wc}) as a function of temperature for various Δ_0, with the variation of T_c with Δ_0 or Γ shown in the inset. One clearly sees the logarithmic divergence is cut-off as Δ_0 increases, leading to a maximum in λ at a particular temperature. Once this maximum falls below unity, no superconducting solution exists.

In order to show that our findings are general and not limited to weak coupling assumptions, we consider a calculation based on a V derived from a phenomenological form for χ[24,25]:

$$V(k, \Omega) = \frac{3}{2} g_{sf}^2 \frac{\chi_{\mathbf{Q}}}{\xi_{AF}^{-2} + 2 + \cos k_x + \cos k_y - i\frac{\Omega}{\Omega_{sf}}} \tag{19}$$

where g_{sf} is the coupling between fermions and spin fluctuations, ξ_{AF} is the antiferromagnetic coherence length, Ω_{sf} is the characteristic spin fluctuation energy scale, and $\chi_{\mathbf{Q}}$ is the static susceptibility at the commensurate vector $\mathbf{Q} = (\pi, \pi)$. For illustrative purposes, we take $g_{sf}^2 \chi_{\mathbf{Q}} = 0.27$ eV, $\xi_{AF} = 10$, $\Omega_{sf} = 0.4$ eV with a cutoff energy for Im χ of 0.4 eV, though we have studied a variety of parameter sets (particularly variation of ξ_{AF}). In general, these parameters are temperature dependent, but for simplicity we ignore this. We use the same model G from above which was used to study the weak coupling limit. Fig. 4a shows the variation of T_c with the pseudogap for different values of Γ. As in the weak coupling case, Δ_0 and Γ suppress T_c. As expected, the size of Δ_0 needed to destroy superconductivity is of order T_{c0}. The behavior of λ with temperature is similar to the weak coupling case, as illustrated in Fig. 4b. Again, a solution fails to appear once the temperature maximum of λ falls below unity. The same behavior was found in the Fermi surface restricted results presented in Fig. 1. In turn, use of our phenomenological G and χ in the full Brillouin zone

formalism leads to similar behavior to Fig. 1 as well, with weakly temperature dependent λ having values much less than unity (see Supplementary Information).

Over much of the doping-temperature phase diagram of the cuprates, ARPES reveals strongly lifetime broadened features with a large pseudogap above T_c. Despite this, T_c is large except under extreme underdoping conditions. The work presented above indicates that for such a large pseudogap, there should be no superconducting solution. In our phenomenological studies, this can be mitigated somewhat by using model Green's functions[21] which have Fermi surfaces in the pseudogap phase (as occurs with charge ordering, spin ordering, or more phenomenological considerations like those of Yang, Rice and Zhang[26]). On the other hand, the fact that we find this same behavior using experimental Green's functions indicates that this is a general issue, not specific to any particular model.

There is a way out of this dilemma. If the pseudogap were due to pairing, then all of the above conclusions are invalidated. In this case, the mean field T_c would actually be the temperature at which Δ_0 becomes non-zero, with the true T_c suppressed from this due to fluctuations. In a preformed pairs picture, T_c would be controlled by the phase stiffness of the pairs[7], whereas in RVB theory, it would be controlled by the coherence temperature of the doped holes[8]. Regardless, our results are in strong support for such models. ARPES[27,28] and tunneling (STM)[29,30] are consistent with a pairing pseudogap, since the observed spectra associated with the antinodal region of the zone have a minimum at zero bias as would be expected if the gap were due to pairing (local or otherwise). This does not mean that charge and/or spin ordering does not occur in the pseudogap phase, it is just that our results are consistent with these phenomena not being responsible for the pseudogap itself.

References

[1] Timusk, T. and Statt, B. The pseudogap in high-temperature superconductors: an experimental survey. Rep. Prog. Phys. **62**, 61 (1999).

[2] Norman, M. R., Pines, D. and Kallin, C. The pseudogap: friend or foe of high T_c? Adv. Phys. **54**, 715 (2005).

[3] Kaminski, A. *et al.* Spontaneous breaking of time reversal symmetry in the pseudogap state of a high-T_c superconductor. Nature **416**, 610 (2002).

[4] Fauque, B. *et al.* Magnetic Order in the Pseudogap Phase of High-T_c Superconductors. Phys. Rev. Lett. **96**, 197001 (2006).

[5] Xia, J. *et al.* Polar Kerr-Effect Measurements of the High-Temperature $YBa_2Cu_3O_{6+x}$ Super-

conductor: Evidence for Broken Symmetry near the Pseudogap Temperature. Phys. Rev. Lett. **100**, 127002 (2008).

[6] Shekhter, A. *et al.* Bounding the pseudogap with a line of phase transitions in $YBa_2Cu_3O_{6+\delta}$. Nature **498**, 75 (2013).

[7] Emery, V. J. and Kivelson, S. A. Importance of phase fluctuations in superconductors with small superfluid density. Nature **374**, 434 (1995).

[8] Lee, P. A., Nagaosa, N. and Wen, X.-G. Doping a Mott insulator: Physics of high-temperature superconductivity. Rev. Mod. Phys. **78**, 17 (2006).

[9] Schrieffer, J. R., Scalapino, D. J. and Wilkins, J. W. Effective tunneling density of states in superconductors. Phys. Rev. Lett. **10**, 336 (1963).

[10] McMillan, W. L. and Rowell, J. M. Lead phonon spectrum calculated from superconducting density of states. Phys. Rev. Lett. **14**, 108 (1965).

[11] Huang, Q. *et al.* Tunnelling evidence for predominantly electron-phonon coupling in superconducting $Ba_{1-x}K_xBiO_3$ and $Nd_{2-x}Ce_xCuO_{4-y}$. Nature **347**, 369 (1990).

[12] Chatterjee, U. *et al.* Dynamic spin-response function of the high-temperature $Bi_2Sr_2CaCu_2O_{8+\delta}$ superconductor from angle-resolved photoemission spectra. Phys. Rev. B **75**, 172504 (2007).

[13] Kaminski, A. *et al.* Renormalization of Spectral Line Shape and Dispersion below T_c in $Bi_2Sr_2CaCu_2O_{8+\delta}$. Phys. Rev. Lett. **86**, 1070 (2001).

[14] Stock, C. *et al.* Spin dynamics near the critical doping in weakly superconducting underdoped $YBa_2Cu_3O_{6.35}$ (T_c=18 K). Phys. Rev. B **77**, 104513 (2008).

[15] Hinkov, V. *et al.* Spin dynamics in the pseudogap state of a high-temperature superconductor. Nature Phys. **3**, 780 (2007).

[16] Monthoux, P. and Pines, D. Spin-fluctuation-induced superconductivity in the copper oxides: A strong coupling calculation. Phys. Rev. Lett. **69**, 961 (1992).

[17] Scalapino, D. J. A common thread: The pairing interaction for unconventional superconductors. Rev. Mod. Phys. **84**, 1383 (2012).

[18] Vilk, Y. M. and Tremblay, A.-M. S. Non-Perturbative Many-Body Approach to the Hubbard Model and Single-Particle Pseudogap. J. Phys. I **7**, 1309 (1997).

[19] Dahm, T. *et al.* Strength of the spin-fluctuation-mediated pairing interaction in a high-temperature superconductor. Nature Phys. **5**, 217 (2009).

[20] Maier, T. A., Jarrell, M. and Scalapino, D. J. Pairing interaction in the two-dimensional Hubbard model studied with a dynamic cluster quantum Monte Carlo approximation. Phys. Rev. B **74**, 094513 (2006).

[21] Norman, M. R., Kanigel, A., Randeria, M., Chatterjee, U. and Campuzano, J. C. Modeling the Fermi arc in underdoped cuprates. Phys. Rev. B **76**, 174501 (2007).

[22] *Handbook of Mathematical Functions*, eds. Abramowitz, M. and Stegun, I. A. (Washington, U.S. Govt. Print. Office, 1964), p. 806, Eq. 23.1.30.

[23] Abrikosov, A. A. and Gorkov, L. P. Contribution to the theory of superconducting alloys with paramagnetic impurities. Sov. Phys. JETP **12**, 1243 (1961).

[24] Millis, A. J. Nearly antiferromagnetic Fermi liquids: An analytic Eliashberg approach. Phys. Rev. B **45**, 13047 (1992).

[25] Abanov, A., Chubukov, A. V. and Schmalian, J. Quantum-critical theory of the spin-fermion model and its application to cuprates: normal state analysis. Adv. Phys. **52**, 119 (2003).

[26] Yang, K.-Y., Rice, T. M. and Zhang, F.-C. Phenomenological theory of the pseudogap state. Phys. Rev. B **73**, 174501 (2006).

[27] Kanigel, A. *et al.* Evidence for pairing above the transition temperature of cuprate supercon-

ductors from the electronic dispersion in the pseudogap phase. Phys. Rev. Lett. **101**, 137002 (2008).

[28] Yang, H.-B. *et al.* Emergence of preformed Cooper pairs from the doped Mott insulating state in $Bi_2Sr_2CaCu_2O_{8+\delta}$. Nature **456**, 77 (2008).

[29] Kohsaka, Y. *et al.* How Cooper pairs vanish approaching the Mott insulator in $Bi_2Sr_2CaCu_2O_{8+\delta}$. Nature **454**, 1072 (2008).

[30] Alldredge, J. W. *et al.* Evolution of the electronic excitation spectrum with strongly diminishing hole density in superconducting $Bi_2Sr_2CaCu_2O_{8+\delta}$. Nature Phys. **4**, 319 (2008).

Acknowledgments

The authors thank Doug Scalapino for suggesting this work, and he and Andrey Chubukov for several helpful discussions. This work was supported by the US DOE, Office of Science, under contract DE-AC02-06CH11357 and by the Center for Emergent Superconductivity, an Energy Frontier Research Center funded by the US DOE, Basic Energy Sciences, under Award No. DE-AC0298CH1088.

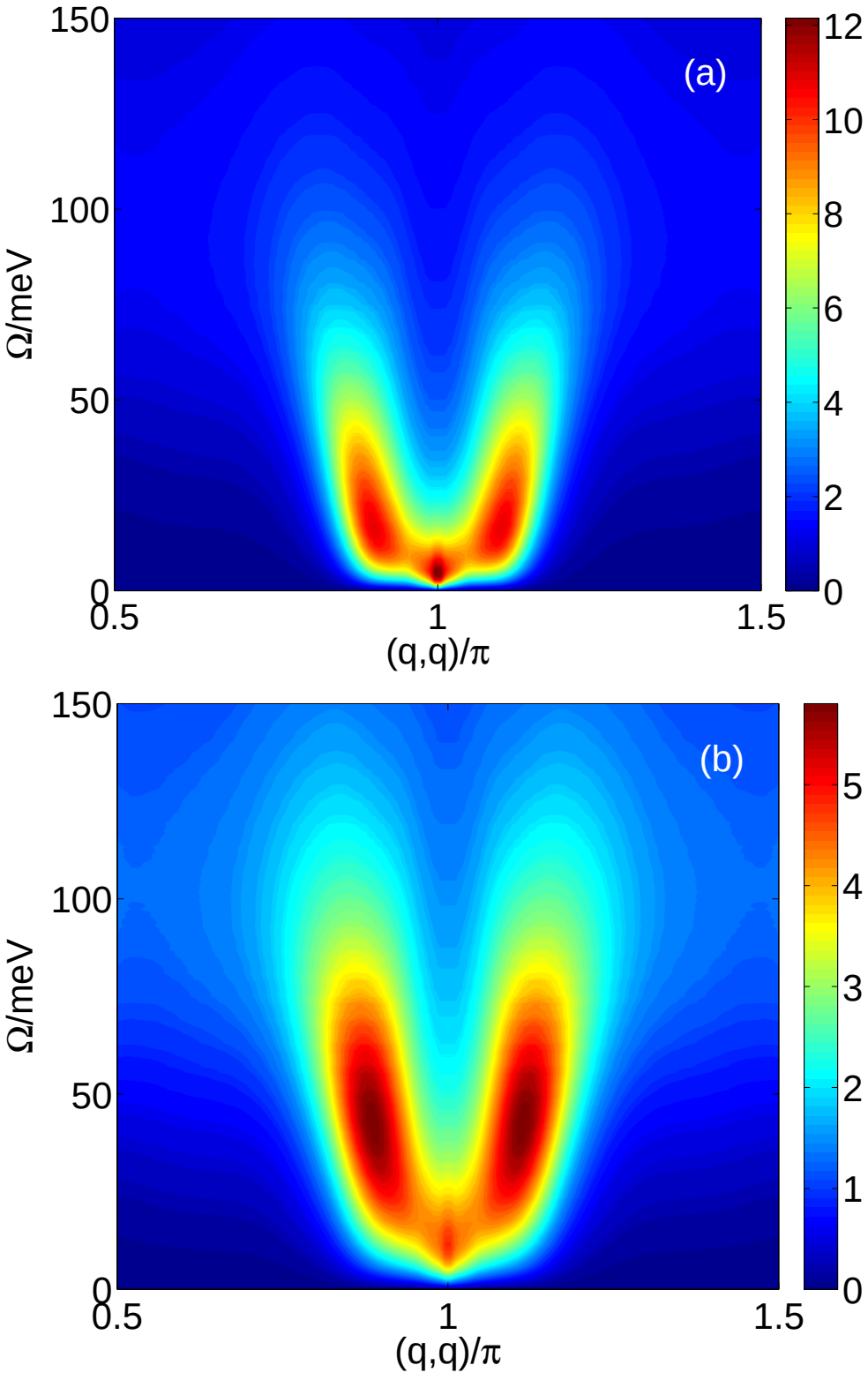

FIG. 1: Imaginary part of the susceptibility χ'' constructed from experimental Green's functions versus energy along the nodal direction for (a) U=860 meV and (b) 800 meV.

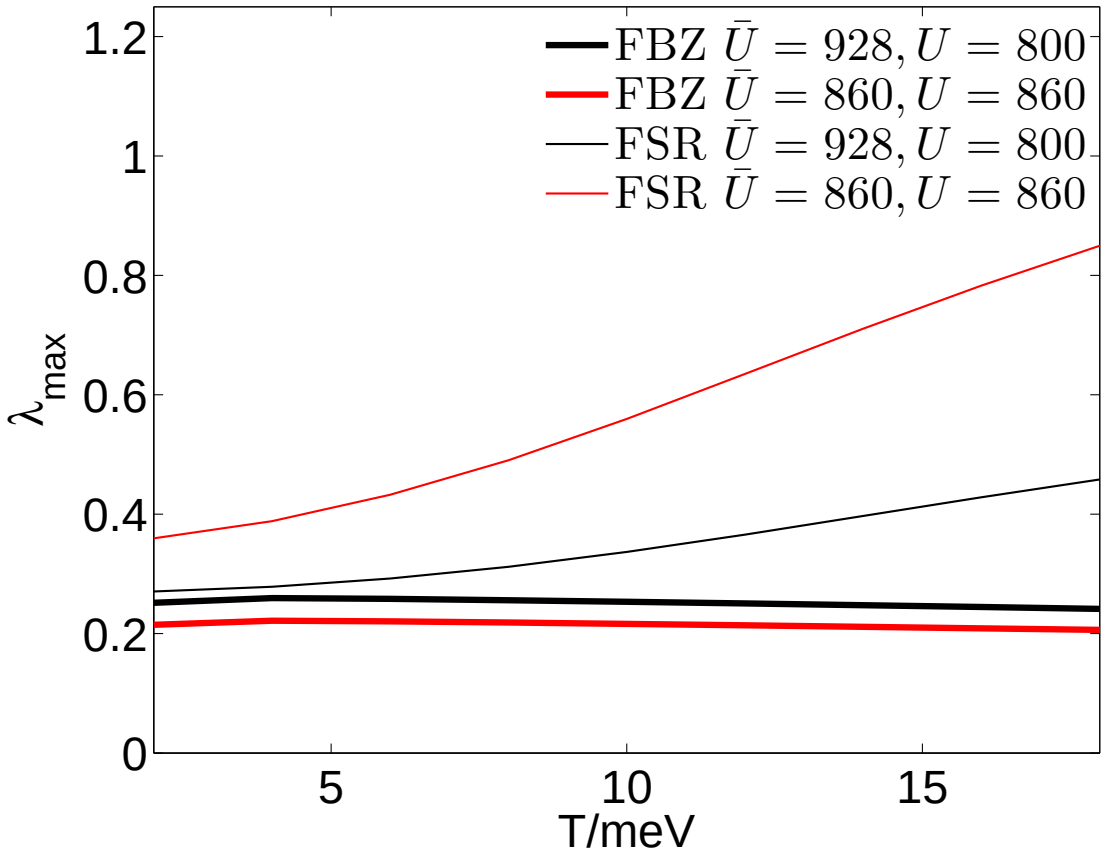

FIG. 2: The leading eigenvalue λ_{max} as a function of temperature, using experimental spectral functions. FSR (thin curves) represent Fermi surface restricted calculations, FBZ (thick curves) represent eigenvalues obtained from Eq. (8) (full Brillouin zone). The interaction parameters are indicated in units of meV.

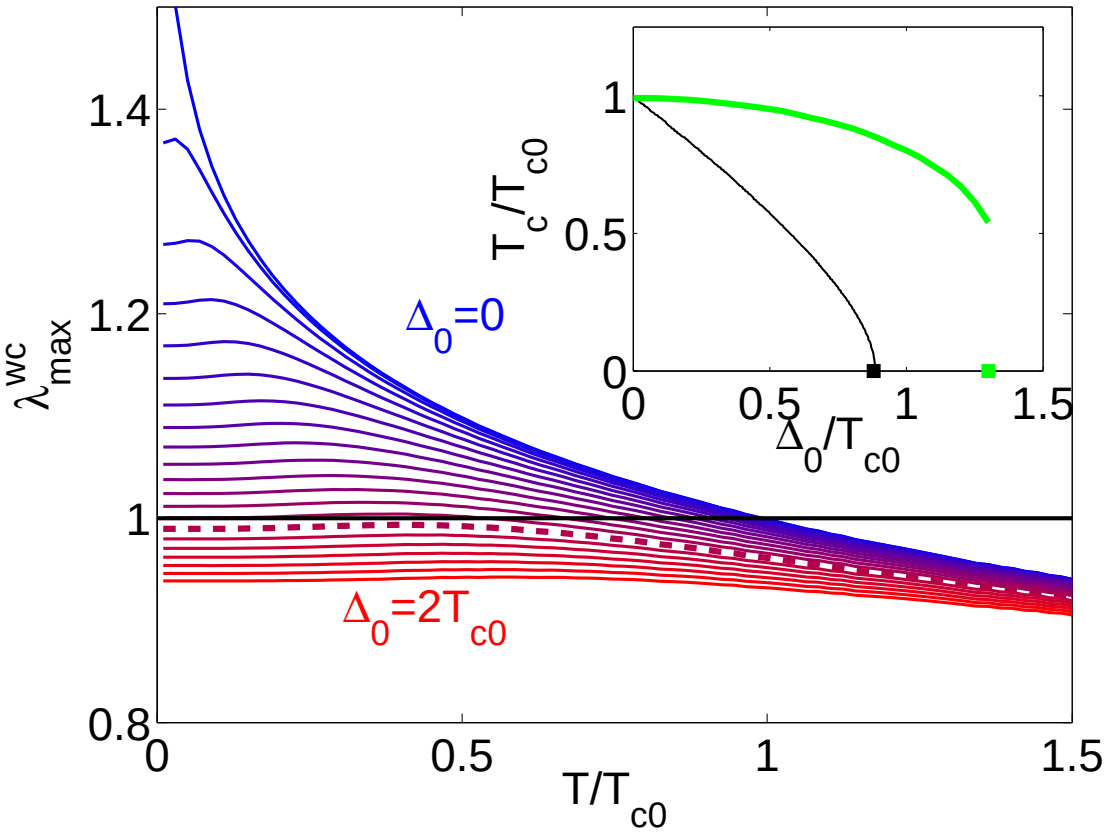

FIG. 3: λ^{wc}_{max} for a d-wave superconductor with a d-wave pseudogap as a function of temperature plotted for various values of the pseudogap. This quantity (left hand side of Eq. (14), with $\Gamma = 0$) is the weak coupling analog of λ_{max}. All energies are normalized to the mean field transition temperature T_{c0} for $\Gamma, \Delta_0 = 0$. For large enough Δ_0, a solution does not exist (dashed curve and ones below it). Inset: T_c as a function of the pseudogap. The curve abruptly terminates when the maximum in λ as a function of T goes below unity. The thin curve shows T_c as a function of the inverse lifetime Γ. In this case, the x axis should be read as Γ/T_{c0}. The filled boxes are the analytic estimates at T=0.

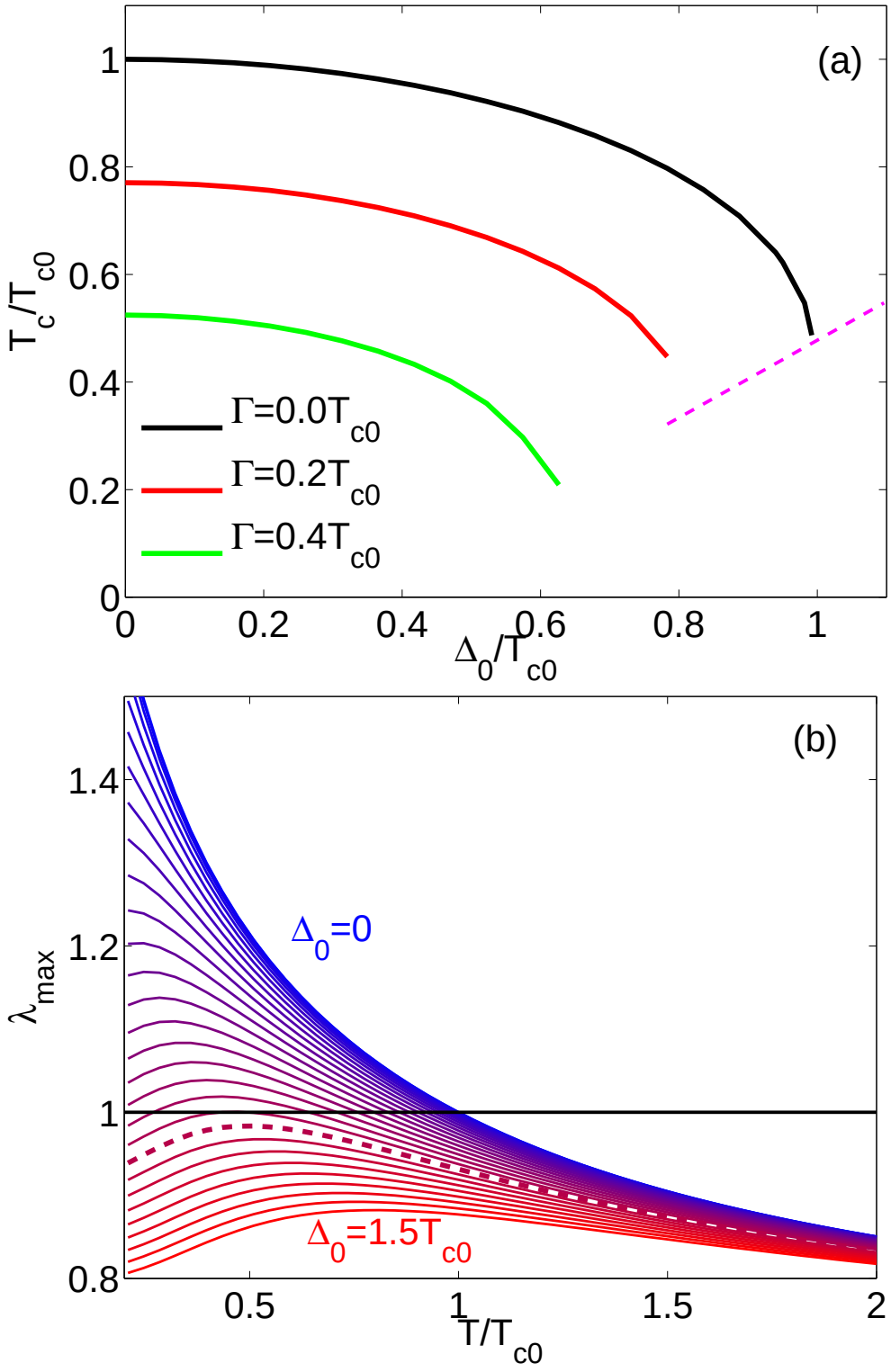

FIG. 4: Transition temperature as a function of the pseudogap Δ_0 for various values of the inverse lifetime Γ (a). The energy scales are normalized to the value of T_{c0} (4.8 meV) for $\Delta_0, \Gamma = 0$. The dashed curve is the variation of the temperature maximum in λ for the $\Gamma = 0$ case. Once the T_c curve intersects this, no solution exists. This is evident from (b), where the temperature dependence of λ_{max} is plotted for various Δ_0. For the dashed curve and below, no solution exists.

Supplementary material

A. Pairing equations

For the full Brillouin zone calculations, we use a 64 by 64 point grid in the first Brillouin zone and a Matsubara cut-off of 40. For the Fermi surface restricted calculations, we use an angular step of 1 degree on the Fermi surface, with a Matsubara cut-off of 100. Convergence was tested for both the k point sum and the Matsubara cut-off. The tight binding fit used for ξ_k was that of Kaminski *et al*[1].

Technically, we should be solving two coupled equations, one for Φ and one for Z. But since we are equating G to the experimental Green's function from ARPES, we do not solve the Z equation. We note that the popular 'trick' of reducing these two equations to a single master equation in the Fermi surface restricted case does not work in the presence of a pseudogap. That is, the pseudogap can be represented in the functional form[2]

$$\Sigma_{PG} = \frac{\Delta_k^2}{\omega - X_k} \tag{20}$$

which can be easily generalized to include broadening. Here, X_k is $-\xi_k$ for the pairing case, and ξ_{k+Q} for density wave ordering at Q. The important point is because of the strong dependence of X_k on $k_\perp$, one cannot collapse to a simple master equation commonly used in Eliashberg calculations[3]. We admit, though, that because we do not solve the Z equation (except to estimate $\bar{U}$), we could be overestimating pair breaking effects.

B. Temperature dependent models

To mimic the temperature dependence of the spectral function, we can allow Γ and Δ_0 to be T dependent in

$$A(k,\omega) = -\frac{1}{\pi} Im \left[\frac{\omega + i\Gamma + \xi_k}{(\omega + i\Gamma)^2 - \xi_k^2 - \Delta_k^2} \right]. \tag{21}$$

Based on the ARPES data, we take Δ_0 to be temperature independent. For the Fermi surface restricted calculations, it has the form $\Delta_0 \cos(2\phi)$ with a Δ_0 of 50 meV. For the full Brillouin zone calculations, it has the form $\Delta_0(\cos(k_x) - \cos(k_y))/2$ with a Δ_0 of 54 meV. In both cases, we again use χ constructed from the experimental Green's functions, and so the A in Eq. (21) is just used in the GG part of the pair vertex. With a temperature

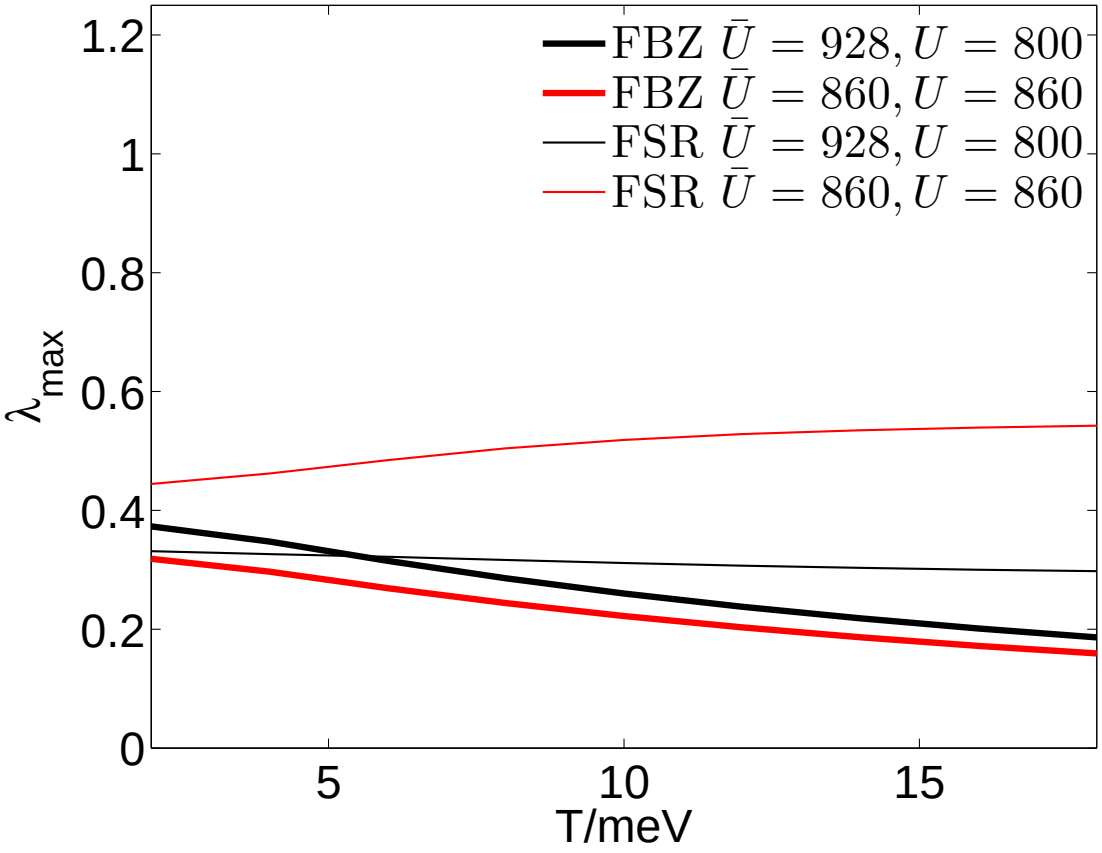

FIG. 5: The leading eigenvalue λ_{max} as a function of temperature, as in Fig. 2, but using for GG the model spectral function of Eq. (21) with a T dependent Γ. The interaction parameters are indicated in units of meV.

independent Γ=50 meV, we find similar behavior in the pairing equation as when we use the experimental spectral functions. Next we consider a more realistic model where Γ behaves linearly with T as in marginal Fermi liquid theory (here, we use a coefficient in front of T of 5.58 to reproduce the pseudogap temperature T* of 180 K for this sample, since this form for G will becomes gapless at the anti-node[2] once $\Gamma = \sqrt{3}\Delta_0$). Again, the behavior of λ_{max} with T is similar to before, as shown in Fig. 5.

References

[1] Kaminski, A. *et al.* Phys. Rev. B **71**, 014517 (2005).

[2] Norman, M. R., Kanigel, A., Randeria, M., Chatterjee, U. and Campuzano, J. C. Phys. Rev. B **76**, 174501 (2007).

[3] Abanov, A., Chubukov, A. V. and Norman, M. R. Phys. Rev. B **78**, 220507 (2008).